Electronic Supplementary Material (ESI) for Physical Chemistry Chemical Physics.

Coherent vibrational modes promote the ultrafast internal conversion and intersystem crossing in thiobases

Danielle Cristina Teles-Ferreira[a,b‡], Ivo HM van Stokkum[c‡], Irene Conti[e], Lucia Ganzer[d], Cristian Manzoni[d], Marco Garavelli[e], Giulio Cerullo[d] , Artur Nenov[e,*], Rocío Borrego-Varillas[d,*] and Ana Maria de Paula[a,*]

1. Spectroscopy of 4TU

Figure S *1* a) reports the 4-thiouracil normalized steady-state absorption (black curve), pump pulse profile (red curve), and the photoluminescence (PL). The panels b), c) and d) detail the 4-thiouracil transient absorption spectroscopy (TAS) [1] which is strongly modulated by coherent oscillations.

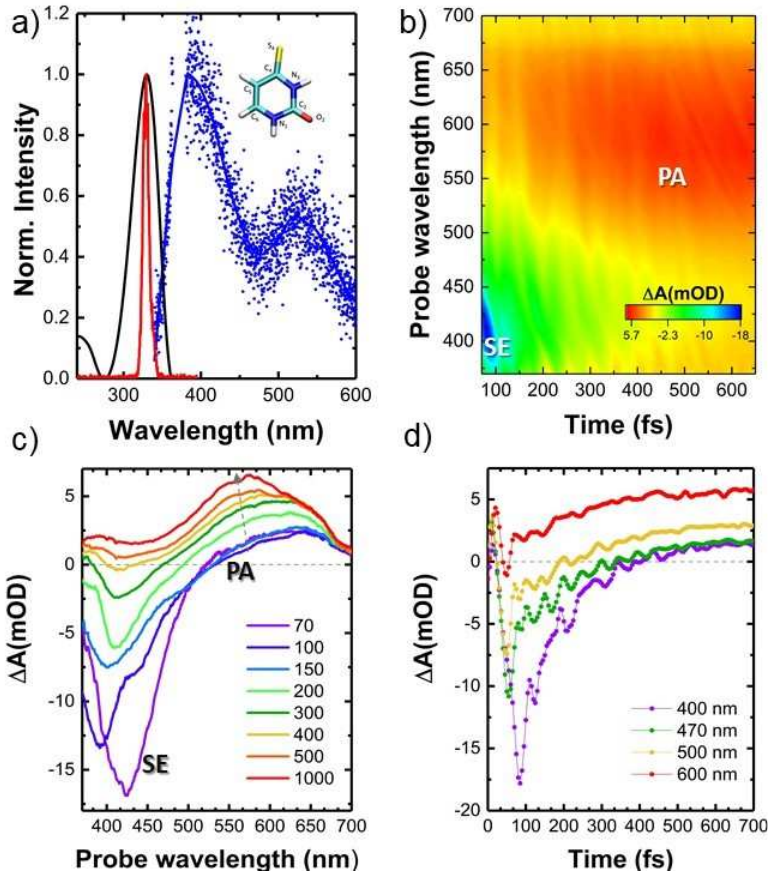

Figure S 1. a) 4-Thiouracil normalized optical absorption intensity (black curve), normalized pulse spectrum intensity used as pump in the TAS experiments (red curve), and normalized PL spectrum intensity (blue curve is the fit and blue dots are the data) obtained with the pump at 330 nm. b) TAS map; c) differential absorption spectra at selected time delays. d) differential absorption dynamics at selected probe wavelengths [1].

2. Energetics at critical points along the relaxation profile

Table S1. *Energies (eV) of the lowest two singlet and triplet state of 4-thiothymidine at representative geometries*

	$Min_{TT}S_0$	**$Min_{TT}S_2$ ($^1\pi\pi^*$)**	**$Min_{TT}S_1$ ($^1\pi\pi^*$)**	**$CI_{TT}S_2/S_1$**	**$Min_{TT}T_1$ ($^1\pi\pi^*$)**	**$Min_{TT}T_2$ ($^1n\pi^*$)**
S_0	0,00	0,54	0,58	0,89	0,29	0,55
S_1 ($^1n\pi^*$)	3,19	3,17	**2,93**	**3,73**	3,15	2,98
S_2 ($^1\pi\pi^*$)	3,88	**3,55**	3,70	**3,79**	3,73	3,71
T_1($^3\pi\pi^*$)		2,91	2,87	0,21	**2,73**	2,89
T_2($^3n\pi^*$)		3,23	3,10		3,21	**3,03**

Table S2. *Energies (eV) of the lowest two singlet and triplet state of 4-thiouracil at representative geometries*

	$Min_{TU}S_0$	**$Min_{TU}S_2$ ($^1\pi\pi^*$)**	**$Min_{TU}S_1$ ($^1\pi\pi^*$)**	**$CI_{TU}S_2/S_1$** (planar)	**$CI_{TU}S_2/S_1$** (twisted)	**$Min_{TU}T_1$ ($^1n\pi^*$)**
S_0	0,00	0,50	0,36	1,19	1,50	0,36
S_1 ($^1n\pi^*$)	2,93	2,82	**2,72**	**3,89**	**4,16**	2,79
S_2 ($^1\pi\pi^*$)	**3,84**	**3,46**	3,63	**4,05**	**4,23**	3,67
T_1 ($^3\pi\pi^*$)	2,90	2,87	2,76			**2,69**
T_2 ($^3n\pi^*$)	3,04	2,95	2,90			2,98

3. Geometric parameters for 4-thiouracil

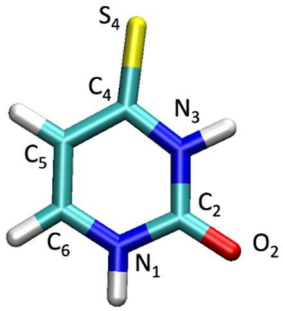

Table S3. *Geometrical parameters of 4-thiouracil at representative geometries*

	FC	Min_{S2}	CI	Min_{S1}	Min_{T1}
N_1C_6 (A)	1.37	1.38	1.32	1.41	1.40
C_5C_6 (A)	1.36	1.42	**1.56**	1.39	1.41
C_4C_5 (A)	1.43	1.38	1.37	1.40	1.40
C_4S_4 (A)	1.66	**1.81**	1.72	1.76	1.73
C_4N_3 (A)	1.38	1.41	1.45	1.41	1.42
C_2N_3 (A)	1.38	1.38	1.34	1.38	1.38
N_1C_2 (A)	1.36	1.38	1.43	1.37	1.37
$N_3C_4S_4$ (°)	120	**112**	112	116	119
C_4N_3H (°)	117	119	**110**	122	120
$O_2C_2N_3$ (°)	123	123	**129**	121	122
HC_5C_6H (°)	0	-4	1	-2	-6
$S_4C_4C_5C_6$ (°)	179	178	179	184	**168**

4. Geometric parameters for 4-ThioThymidine

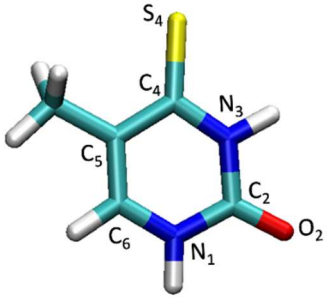

Table S4. *Geometrical parameters of 4-thiothymidine at representative geometries*

	FC	Min_{S2}	CI	Min_{S1}	Min_{T1}
N_1C_6 (A)	1.39	1.39	1.34	1.41	1.40
C_5C_6 (A)	1.37	1.40	**1.50**	1.39	1.44
C_4C_5 (A)	1.44	1.39	1.37	1.40	1.39
C_4S_4 (A)	1.66	**1.83**	1.75	1.76	1.71
C_4N_3 (A)	1.39	1.40	1.44	1.41	1.41
C_2N_3 (A)	1.39	1.39	1.35	1.39	1.38
N_1C_2 (A)	1.39	1.39	1.45	1.38	1.39
$N_3C_4S_4$ (°)	122	**114**	118	112	119
C_4N_3H (°)	118	119	116	120	120
$O_2C_2N_3$ (°)	122	122	**127**	121	122
$H_3CC_5C_6H$ (°)	-1	2	**-24**	-7	-4
$S_4C_4C_5C_6$ (°)	179	**193**	181	**157**	180

5. Normal mode analysis

To obtain a better idea of the ES vibrational dynamics of 4-ThioUracil (4TU) and 4-ThioThymidine (4TT) we performed a normal mode analysis. To this aim:

a) S_2 normal modes were used to project geometrical deformations from the FC to the S_2 minimum
b) S_2 normal modes were used to project geometrical deformations from the S_2 minimum to the CI(S_2/S_1);
c) S1 normal modes were used to project the dynamics in the S1 state from the CI towards the corresponding minimum;
d) T1 normal modes were used to study the geometrical deformation from the S1 minimum to the T1 minimum.

Starting from the definition of the normal mode matrix

$$\mathbb{P}^{\dagger} = \mathbb{M}^{\frac{1}{2}} \nabla_{\tilde{\boldsymbol{q}}} \boldsymbol{Q}$$

where $\mathbb{P}$ is a matrix whose columns are the normal modes of the system $\tilde{\boldsymbol{q}}_k$ expressed in normalized mass-weighted Cartesian coordinates $\boldsymbol{Q}$ and $\mathbb{M}$ is a diagonal matrix with the nuclear masses, one can reformulate it in terms of finite differences

$$\mathbb{P}^{\dagger} \Delta \tilde{\boldsymbol{q}} = \mathbb{M}^{\frac{1}{2}} \Delta \boldsymbol{Q}$$

Thus, $\Delta \tilde{\boldsymbol{q}}$ represents the array of unitless displacements $\tilde{\boldsymbol{d}}$ along the normal modes of the system when the difference is taken with respect to the reference point on the i-the electronic state. Rearranging gives the final working equation

$$\tilde{\boldsymbol{d}}_i = \mathbb{P}^{-1} \mathbb{M}^{\frac{1}{2}} \Delta \boldsymbol{Q}$$

which allows to estimate how much every normal mode $\tilde{\boldsymbol{q}}_k$ has to be displaced to connect two points in Cartesian coordinate space of the potential energy surface of the i-th electronic state. $\Delta \boldsymbol{Q}$ is the

difference in Cartesian coordinates between two geometries. The displacements $\tilde{\boldsymbol{d}}_i$ can be related to spectroscopic parameters like the Huang-Rhys factors S_{ik} or the reorganization energy λ_{ik} of the system:

$$S_{ik} = \frac{\tilde{d}_{ik}^2 \omega_k}{2\hbar} \text{ and } \qquad \lambda = \frac{\tilde{d}_{ik}^2 \omega_k^2}{2\hbar}$$

where ω_k is the frequency of the k-th normal mode.
With the normal mode analysis attention should be paid to global translational and rotational degrees of freedom which have to be removed prior to computing the difference in Cartesian coordinates. To this end we followed an iterative procedure relying on the vectors of inertia in order to minimize the distance in space between two geometries as outlined in ref. [Kurtz, L. Dissertation at the LMU Muenchen, 2001.].

In Tables 5 and 6 we list the normal modes (below 2000 cm^{-1})[1] and reorganization energies (in cm^{-1}) along the FC→T_1 path (following a)-d)) for 4TU and 4TT. Note that for 4TT the entire nucleoside was considered in the calculation of the normal modes. For the sake of a better comparison in Table 7 we also report normal mode analysis on 4TT based on normal modes and frequencies computed only for the 4-thiothymine chromophore. Color code is used to label normal modes with significant reorganization energies for modes with frequencies below 1000 cm^{-1} (i.e. modes which can be resolved with our experimental set up) Normal modes which are observed experimentally following our analysis are highlighted.
The total reorganization energy resulting from the projection is compared with the QMMM energy difference between the two geometries. The values show reasonable agreement and demonstrate the stability and reliability of the projection procedure. The only discrepancy is observed for the distortion leading from the S_2 minimum to the $CI_{TT}(S_2/S_1)$ of 4TT where the normal mode projection predicts triple increase in reorganization energy with respect to the QMMM value. This is due to the large geometrical deformation towards the CI (i.e. methyl out-of-plane) which breaks the harmonic approximation in which the normal modes are defined.

[1] High frequency C-H, N-H and O-H stretchings are not involved in the structural deformations and are thus left out

4-thioUracil

Table S5. Reorganization energies λ [cm^{-1}] along the normal modes of 4TU along the deformations FC→Min_{S2}, Min_{S2}→CI, CI→Min_{S1} and Min_{S1}→Min_{T1}. Color code is used to label modes with notable reorganization energies below 1000 cm^{-1}.

FC → Min_{S2}				Min_{S2} → CI			CI → Min_{S1}			Min_{S1} → Min_{T1}		
Mode	ω [cm^{-1}]	λ [cm^{-1}]		Mode	ω [cm^{-1}]	λ [cm^{-1}]	Mode	ω [cm^{-1}]	λ [cm^{-1}]	Mode	ω [cm^{-1}]	λ [cm^{-1}]
1	122.1	1		1	122.1	3	1	121.4	8	1	115.9	39
2	180.3	11		2	180.3	26	2	138.6	13	2	179.2	90
3	226.2	80	S in-plane bending	3	226.2	1	3	213.4	20	3	220.2	210
4	259.3	0		4	259.3	16	4	222.8	176	4	279.5	101
5	387.2	407	breathing along the S_4C_4--N_1H axis	5	387.2	87	5	400.2	0	5	408.9	0
6	425.3	7		6	425.3	0	6	427.4	21	6	443.6	1
7	491.5	202	O in-plane bending	7	491.5	353	7	486.7	759	7	495.3	1
8	538.1	11		8	538.1	37	8	519.2	10	8	551.8	16
9	564	3		9	564	7	9	575.2	4	9	596.9	2
10	646.4	1		10	646.4	0	10	611.3	29	10	634.4	12
11	675	1016	breathing along the HC_6--N_3H axis	11	675	9	11	689.1	42	11	704	0
12	702.9	37		12	702.9	7	12	700.8	0	12	714	2
13	791.9	5		13	791.9	10	13	737.8	23	13	766.6	6
14	846	0		14	846	54	14	797.4	68	14	800.1	1
15	902.3	13	C_4-S_4 stretching	15	902.3	629	15	944.6	162	15	929.7	37
16	990	38		16	990	498	16	987.9	317	16	991.2	4
17	1011.3	585		17	1011.3	492	17	1043.4	188	17	1037.8	30
18	1052.3	2		18	1052.3	519	18	1139.5	767	18	1114.3	18
19	1202.8	15		19	1202.8	29	19	1208.5	147	19	1223.2	0
20	1297	11		20	1297	0	20	1305.9	8	20	1302.6	14
21	1317.9	74		21	1317.9	940	21	1381.2	2187	21	1352.8	15
22	1413.5	593		22	1413.5	169	22	1442.3	1794	22	1445.7	17
23	1430.4	29		23	1430.4	86	23	1469.8	277	23	1481.1	0
24	1514.1	99		24	1514.1	1	24	1506.5	493	24	1508.7	0
25	1539.3	443		25	1539.3	113	25	1528.8	1138	25	1552.7	6
26	1767	11		26	1767	17	26	1756.7	39	26	1764.2	0

λ (proj) [cm^{-1}]	3694	λ (proj) [cm-1]	4103	λ (proj) [cm-1]	8690	λ (proj) [cm-1]	622
ΔE [cm^{-1}]	3710	ΔE [cm-1]	3952	ΔE [cm-1]	9597	ΔE [cm-1]	645

4-thioThymidine

Table S6. Reorganization energies λ [cm^{-1}] along the normal modes of 4TT along the deformations FC→Min_{S2}, Min_{S2}→CI, CI→Min_{S1} and Min_{S1}→Min_{T1} using the normal modes of the nucleoside. Color code is used to label modes with notable reorganization energies below 1000 cm^{-1}. Mixing of energetically close lying modes involving the chromophore and the sugar leading to the chromophore deformations being present in two or three modes.

FC → Min_{S2}				Min_{S2} → CI			CI → Min_{S1}			Min_{S1} → Min_{T1}		
Mode	ω [cm^{-1}]	λ [cm^{-1}]		Mode	ω [cm^{-1}]	λ [cm^{-1}]	Mode	ω [cm^{-1}]	λ [cm^{-1}]	Mode	ω [cm^{-1}]	λ [cm^{-1}]
1	66.1	0		1	66.1	0	1	-43.2	0	1	64.6	0
2	75.2	0		2	75.2	0	2	63	0	2	81.5	0
3	80.6	0		3	80.6	0	3	97	0	3	89.6	0
4	119.2	14		4	119.2	37	4	102.7	1	4	119.7	16
5	127.1	7		5	127.1	9	5	119.5	32	5	125.3	75
6	138.7	6		6	138.7	75	6	137.4	6	6	141.5	1
7	163.9	48	S out-of-plane (OOP) + CH3 OOP	7	163.9	134	7	150.9	175	7	156.3	43
8	171.7	1		8	171.7	4	8	158.4	48	8	166.5	19
9	196.7	0		9	196.7	14	9	192	5	9	193.8	0
10	224.4	13	S in-plane bending	10	224.4	24	10	209.1	222	10	225.4	31
11	243.8	10		11	243.8	2	11	238	73	11	242.1	75
12	264.7	82		12	264.7	188	12	261.4	311	12	257.3	363
13	268.2	61		13	268.2	16	13	280	275	13	278.3	2
14	295	36		14	295	8	14	296.3	76	14	292.3	3
15	314.1	8	CH_3 in-plane bending	15	314.1	130	15	312.3	409	15	326.6	52
16	356.8	19		16	356.8	3	16	345.8	23	16	347.9	14
17	361.6	18		17	361.6	3	17	363.2	12	17	363.1	6
18	420.1	109	N1, H(N3)& H(C6) OOP	18	420.1	74	18	397.8	2	18	398.4	0
19	426.2	213	breathing along the S_4C_4--N_1H axis + CH_3 in-plane bending	19	426.2	45	19	446.7	24	19	423.5	5
20	473.1	51		20	473.1	59	20	486.8	2	20	444.5	4
21	492	169	breathing along the	21	492	78	21	499.4	72	21	451.7	61

22	504	0	H_3C_5--C_2O_2 axis	22	504	26	22	506.4	58	22	488.4	4
23	517.7	36		23	517.7	67	23	517.9	19	23	503.1	2
24	550.2	28		24	550.2	43	24	532.7	103	24	521	3
25	557.3	0		25	557.3	182	25	562.8	235	25	533.1	0
26	620.3	234	O in-plane bending + C_6 pyramidalization	26	620.3	10	26	612.8	166	26	556.4	0
27	643.1	38		27	643.1	0	27	635.6	253	27	611.3	1
28	657.2	282	breathing along the HC_6--N_3H axis	28	657.2	0	28	641.9	0	28	642.9	2
29	675.8	267		29	675.8	333	29	691.6	6	29	689.5	0
30	727.4	76		30	727.4	6	30	708	0	30	716.5	9
31	735.4	4		31	735.4	67	31	710.9	9	31	733	1
32	754.7	0		32	754.7	0	32	734	16	32	742	0
33	766.5	0		33	766.5	5	33	767.6	5	33	774.6	0
34	837.7	6		34	837.7	74	34	834.3	185	34	838.3	5
35	856.4	2		35	856.4	26	35	855.7	53	35	853	1
36	893.5	4		36	893.5	27	36	887.3	2	36	878.9	67
37	905.5	8		37	905.5	141	37	908.8	171	37	906.7	0
38	962.3	5		38	962.3	10	38	961	253	38	960	32
39	985.2	278	C_4-S_4 stretching	39	985.2	147	39	993.7	9	39	988.3	130
40	1003.7	348		40	1003.7	171	40	1010.1	0	40	994.1	26
41	1008.7	0		41	1008.7	0	41	1029.8	0	41	1009.8	0
42	1030.6	9		42	1030.6	12	42	1033.5	10	42	1030.3	0
43	1043.9	16		43	1043.9	141	43	1053.1	0	43	1040.4	0
44	1054.1	5		44	1054.1	26	44	1056.6	0	44	1041.6	24
45	1057	2		45	1057	0	45	1079.1	0	45	1051.9	0
46	1080.8	0		46	1080.8	1	46	1086.2	31	46	1081.6	0
47	1101	3		47	1101	24	47	1105.6	37	47	1099.6	0
48	1187.3	2		48	1187.3	473	48	1202.6	0	48	1205.3	10
49	1211.4	0		49	1211.4	1	49	1210.4	71	49	1211.9	0
50	1232.1	0		50	1232.1	127	50	1244.2	6	50	1240.7	0
51	1244.4	0		51	1244.4	1	51	1260.3	92	51	1248	64
52	1294	0		52	1294	4	52	1295.9	43	52	1273.1	0
53	1308	66		53	1308	0	53	1311.4	48	53	1296.6	0
54	1314.7	3		54	1314.7	7	54	1317.6	18	54	1317	1

55	1335.6	95
56	1344.7	33
57	1360.6	0
58	1405.1	34
59	1406.5	27
60	1411.2	269
61	1429.6	45
62	1434.7	58
63	1461.1	232
64	1473.4	18
65	1485.5	18
66	1492.9	53
67	1502.9	3
68	1514	40
69	1533.3	0
70	1576.3	59
71	1580.7	1
72	1731.1	0
73	1782.8	0
λ (proj) [cm-1]		3572
ΔE [cm-1]		2742

55	1335.6	659
56	1344.7	111
57	1360.6	0
58	1405.1	26
59	1406.5	7
60	1411.2	40
61	1429.6	15
62	1434.7	31
63	1461.1	1
64	1473.4	6
65	1485.5	21
66	1492.9	66
67	1502.9	5
68	1514	221
69	1533.3	0
70	1576.3	236
71	1580.7	7
72	1731.1	22
73	1782.8	71
λ (proj) [cm-1]		**4600**
ΔE [cm-1]		1694

55	1338.9	17
56	1350.2	31
57	1380.6	718
58	1404	0
59	1404.9	151
60	1412.9	33
61	1433.9	272
62	1448.2	27
63	1451.4	0
64	1472.1	98
65	1483.6	3
66	1488.3	9
67	1503.1	21
68	1520	208
69	1534.6	0
70	1573.7	570
71	1583.8	5
72	1741.7	12
73	1766.5	175
λ (proj) [cm-1]		6017
ΔE [cm-1]		6694

55	1340.1	1
56	1358.4	1
57	1369.5	178
58	1391.9	0
59	1401.2	13
60	1405.2	1
61	1413.9	6
62	1442.7	11
63	1452.7	6
64	1484.3	2
65	1485.2	0
66	1492.5	27
67	1504.6	0
68	1531.6	0
69	1539	8
70	1581.4	0
71	1608.9	45
72	1727.4	1
73	1779.4	2
λ (proj) [cm-1]		1454
ΔE [cm-1]		1613

4-thioThymine (thymine only)

Table S7. Reorganization energies λ [cm^{-1}] along the normal modes of 4TT along the deformations FC→Min_{S2}, Min_{S2}→CI, CI→Min_{S1} and Min_{S1}→Min_{T1} using the normal modes of the 4-ThioThymine chromophore. Color code is used to label modes with notable reorganization energies below 1000 cm^{-1}

FC → Min_{S2}				**Min_{S2} → CI**			**CI → Min_{S1}**			**Min_{S1} → Min_{T1}**		
Mode	ω [cm^{-1}]	λ [cm^{-1}]		Mode	ω [cm^{-1}]	λ [cm^{-1}]	Mode	ω [cm^{-1}]	λ [cm^{-1}]	Mode	ω [cm^{-1}]	λ [cm^{-1}]
1	111.4	18		1	111.4	401	1	-37.5	0	1	100.1	44
2	157	61		2	157	0	2	129.8	17	2	164.9	58
3	208.5	98	S out-of-plane (OOP) + CH_3 OOP	3	208.5	0	3	200.1	265	3	170.4	338
4	233.1	29	S in-plane bending	4	233.1	7	4	218.4	1869	4	256.6	484
5	258.9	81		5	258.9	317	5	281.9	243	5	277.4	18
6	304.9	0	CH_3 in-plane bending	6	304.9	130	6	317.2	358	6	333	277
7	392.6	65	N_1, H(N_3)& H(C_6) OOP	7	392.6	73	7	348	192	7	334.7	106
8	470.6	14		8	470.6	93	8	490.2	28	8	421.8	33
9	493.4	801	breathing along the S_4C_4--N_1H axis + CH_3 in-plane bending	9	493.4	201	9	505.4	4	9	451.7	41
10	502.2	196	breathing along the CH_3C_5--C_2O_2 axis	10	502.2	203	10	514	244	10	490.5	9
11	559.9	41		11	559.9	177	11	554.1	51	11	530.9	8
12	605.6	69	O in-plane bending + C_6 pyramidalization	12	605.6	15	12	625.5	492	12	544.1	1
13	668.3	1		13	668.3	296	13	639.8	123	13	621	46
14	699.7	513	breathing along the HC_6--N_3H axis	14	699.7	70	14	706	37	14	712.7	2
15	735	1		15	735	60	15	723.3	0	15	721.6	4
16	861.9	4		16	861.9	136	16	858.8	109	16	854.9	18
17	994.8	685	C_4-S_4 stretching	17	994.8	474	17	1031.4	0	17	956.1	273
18	1029.5	4		18	1029.5	39	18	1055.4	0	18	1039.4	10
19	1056.5	1		19	1056.5	0	19	1061.9	4	19	1040.7	5
20	1152.8	1		20	1152.8	559	20	1202.6	3	20	1203.7	4
21	1228.3	0		21	1228.3	71	21	1235.1	160	21	1225.4	8

22	1313.5	34	22	1313.5	17	22	1313.6	53	22	1265.4	24
23	1346	232	23	1346	876	23	1377.4	400	23	1365.7	79
24	1406.4	379	24	1406.4	128	24	1412.7	331	24	1390	211
25	1426.8	57	25	1426.8	1	25	1429.5	568	25	1404.1	0
26	1442.8	0	26	1442.8	32	26	1461.2	97	26	1481.5	26
27	1489	0	27	1489	108	27	1486.1	1	27	1485	2
28	1499.4	224	28	1499.4	56	28	1492.8	54	28	1495.3	7
29	1516.3	138	29	1516.3	101	29	1519.8	184	29	1576.9	7
30	1625.3	9	30	1625.3	263	30	1637.2	390	30	1620.8	28
31	1776.9	1	31	1776.9	76	31	1759.1	276	31	1773.1	1
λ (proj) [cm-1]		3757	λ (proj) [cm-1]		**4980**	λ [cm-1]		6553	λ (proj) [cm-1]		2172
ΔE [cm-1]		2742	ΔE [cm-1]		1694	ΔE [cm-1]		6694	ΔE [cm-1]		1613

6. Cartesian Coordinates

4-ThioThymidine

$Min_{TT}S_0$

S	23.752890	18.541599	16.690311
O	21.924515	22.800902	18.400704
N	21.276583	20.896015	19.570888
N	22.649513	20.740406	17.707719
C	21.341791	19.515323	19.683423
C	21.939696	21.576835	18.559874
C	22.082331	18.725396	18.846091
C	22.803227	19.365467	17.772326
C	22.127104	17.235775	19.018651
H	20.750659	19.066957	20.484038
H	23.136015	21.236719	16.955675
H	23.162929	16.897032	19.177031
H	21.755018	16.740124	18.108320
H	21.510541	16.933016	19.875209
H	20.757128	21.433165	20.257262

$Min_{TT}S_2$ ($^1\pi\pi^*$)

S	23.710825	18.493821	16.571236
O	21.923713	22.810992	18.388262
N	21.269787	20.911996	19.564861
N	22.658333	20.741932	17.707866
C	21.283462	19.526131	19.703303
C	21.943607	21.586625	18.550960
C	22.083329	18.721573	18.878881
C	22.859159	19.372992	17.926907
C	22.092601	17.226683	19.046005
H	20.685385	19.100399	20.508385
H	23.227273	21.223226	17.004898
H	23.117077	16.845698	19.176191
H	21.668054	16.743322	18.150877
H	21.492133	16.943031	19.919577
H	20.751715	21.464930	20.242240

$Min_{TT}S_1$ ($^1n\pi^*$)

S	24.089311	18.714155	16.892706
O	21.899163	22.794057	18.422163
N	21.286232	20.875015	19.581584
N	22.681120	20.768402	17.720510
C	21.297059	19.466786	19.671134
C	21.939599	21.566420	18.580771
C	22.021493	18.691811	18.779656
C	22.696742	19.358801	17.746796
C	22.126349	17.200229	18.954850
H	20.685672	19.018464	20.452739
H	22.945317	21.262399	16.865695
H	23.152322	16.912412	19.243450

H	21.871722	16.670880	18.022540
H	21.440425	16.859077	19.741538
H	20.771596	21.410172	20.270634

Min$_{TT}$T$_2$ (^{3}nπ*)

S	24.045594	18.614726	16.948133
O	21.872110	22.798223	18.401501
N	21.277292	20.885912	19.576503
N	22.660382	20.774066	17.709127
C	21.306128	19.482661	19.682081
C	21.920645	21.571054	18.561114
C	22.024018	18.701962	18.777568
C	22.686563	19.362980	17.728549
C	22.112686	17.209913	18.962786
H	20.660103	19.030069	20.432429
H	22.969053	21.279257	16.878090
H	23.036169	16.929923	19.496514
H	22.117321	16.700306	17.985505
H	21.255517	16.846023	19.545422
H	20.766743	21.424089	20.265264

Min$_{TT}$T$_1$ (^{3}$\pi\pi$*)

S	23.847856	18.561173	16.714621
O	21.939361	22.807843	18.432793
N	21.288471	20.900428	19.585914
N	22.695705	20.771408	17.731673
C	21.309480	19.507621	19.711844
C	21.971428	21.579803	18.578140
C	22.133655	18.716500	18.839168
C	22.849134	19.369474	17.836178
C	22.142240	17.231911	19.053104
H	20.652469	19.049622	20.446836
H	23.195390	21.276615	17.000914
H	22.939571	16.746053	18.479806
H	21.168250	16.816401	18.743711
H	22.277775	17.015346	20.122900
H	20.766214	21.445878	20.263525

CI$_{TT}$S$_2$/S$_1$

S	23.540166	18.468942	16.437704
O	21.972477	22.797640	18.463191
N	21.302808	20.862378	19.570262
N	22.482803	20.731867	17.557592
C	21.236563	19.525989	19.685206
C	21.959386	21.562337	18.487718
C	22.055690	18.691929	18.748666
C	22.583006	19.299389	17.642687
C	22.209108	17.265253	19.146108
H	20.481775	19.094566	20.349986

H	22.935522	21.174274	16.752828
H	22.592594	17.220923	20.180027
H	22.905974	16.765023	18.465159
H	21.226557	16.760675	19.131795
H	20.819156	21.425586	20.269306

4-ThioUracil

Min$_{TU}$S$_0$

C	17.803042	18.030324	16.491376
N	18.661627	17.002731	16.231633
C	18.410827	16.057710	15.278065
C	17.318758	16.138658	14.477283
C	16.426965	17.250824	14.598700
N	16.752104	18.128950	15.609377
H	17.124179	15.377005	13.740260
S	15.077605	17.502492	13.673507
O	17.941570	18.789844	17.447464
H	19.124280	15.250151	15.226637
H	16.118840	18.911060	15.770608
H	19.485141	16.940630	16.830954

Min$_{TU}$S$_2$($^1\pi\pi^*$)

C	17.841461	18.030227	16.523073
N	18.697262	16.992647	16.246535
C	18.486346	15.999033	15.300379
C	17.327340	16.110150	14.482429
C	16.493812	17.190969	14.664435
N	16.797775	18.168909	15.620994
H	17.097003	15.354621	13.731320
S	14.984360	17.605527	13.741444
O	17.983607	18.769867	17.513441
H	19.197703	15.176184	15.300475
H	16.105595	18.905578	15.812271
H	19.516149	16.941708	16.879378

CI$_{TU}$S$_2$/S$_1$ (planar)

C	17.823628	18.004384	16.604253
N	18.641189	16.877650	16.268697
C	18.442081	15.910003	15.389424
C	17.190553	16.149969	14.484956
C	16.409320	17.257645	14.701938
N	16.797610	18.174037	15.757071
H	16.971291	15.439154	13.684874
S	15.005230	17.806608	13.866585
O	18.147040	18.679691	17.609426
H	19.174197	15.099225	15.335198
H	16.113357	18.941564	15.833937
H	19.476749	16.876242	16.902826

$CI_{TU}S_2/S_1$ (twisted)

C	17.775866	17.958065	16.605199
N	18.590330	16.798769	16.362939
C	18.456784	15.923791	15.374630
C	17.167055	16.125029	14.531413
C	16.461532	17.358758	14.579890
N	16.944524	18.288548	15.607065
H	16.796598	15.307434	13.917903
S	14.989979	17.725329	13.902948
O	18.003918	18.583541	17.658927
H	19.340878	15.354359	15.086153
H	16.256718	19.036039	15.798897
H	19.408063	16.756509	17.013222

$Min_{TU}S_1(^1n\pi^*)$

C	17.783876	18.018210	16.487077
N	18.680944	17.024615	16.215161
C	18.502802	16.063421	15.210466
C	17.398420	16.167166	14.371364
C	16.521098	17.250044	14.525337
N	16.738543	18.146136	15.593152
H	17.208777	15.401308	13.619063
S	14.952972	17.351192	13.742883
O	17.886569	18.763153	17.479225
H	19.207094	15.237241	15.206599
H	16.110933	18.935102	15.774565
H	19.483656	16.972405	16.857698

$Min_{TU}T_1(^3\pi\pi^*)$

C	17.807640	18.044956	16.472812
N	18.699231	17.032994	16.224927
C	18.491513	16.023161	15.278067
C	17.296346	16.059246	14.532425
C	16.425906	17.143459	14.669849
N	16.795806	18.195080	15.541649
H	17.043039	15.237464	13.861482
S	15.101769	17.384834	13.584329
O	17.913509	18.793336	17.461401
H	19.177048	15.180298	15.303264
H	16.109007	18.919046	15.780443
H	19.504517	16.995436	16.869577

7. DOAS and Target Analyses

The superposition model for the Time Resolved Spectra $TRS(t,\lambda)$ is given by the matrix formula [2]:

$$TRS = C^S(\theta,\mu,\Delta)\cdot SADS^T + \mathrm{Cos}(\omega,\gamma,\mu,\Delta)\cdot A^T + \mathrm{Sin}(\omega,\gamma,\mu,\Delta)\cdot B^T + IRF(\mu,\Delta')\cdot IRFAS^T$$

where the populations C^S are determined by an unknown compartmental model (e.g. Figure S 2), which depends upon the unknown kinetic parameters θ . A Gaussian shaped IRF is used, with parameters μ for the time of the IRF maximum and Δ for the full width at half maximum (FWHM) of the IRF. The matrices $\mathrm{Cos}(\omega,\gamma,\mu,\Delta)$ and $\mathrm{Sin}(\omega,\gamma,\mu,\Delta)$ contain the damped oscillations, and the matrices A and B comprise their amplitudes. In order to limit the number of free parameters, we assume wavelength independence of the eigenfrequency ω_n and of the damping rate γ_n.

The final term, which describes the coherent artefact, contains a matrix $IRF(\mu,\Delta')$ with the zeroth, first and second derivative of the IRF [3]. Experimentally we found that the width $\Delta' > \Delta$. Associated with each IRF derivative are the columns of the *IRFAS* matrix. The "coherent artefact" (CA) is described by the $IRF(\mu,\Delta')\cdot IRFAS^T$ term. It is clearly visible in the traces at 510 and 601 nm in Figure S 3H,I and Figure S 4H,I, with large contributions of the IRF derivatives (Figure S 3D and Figure S 4D).

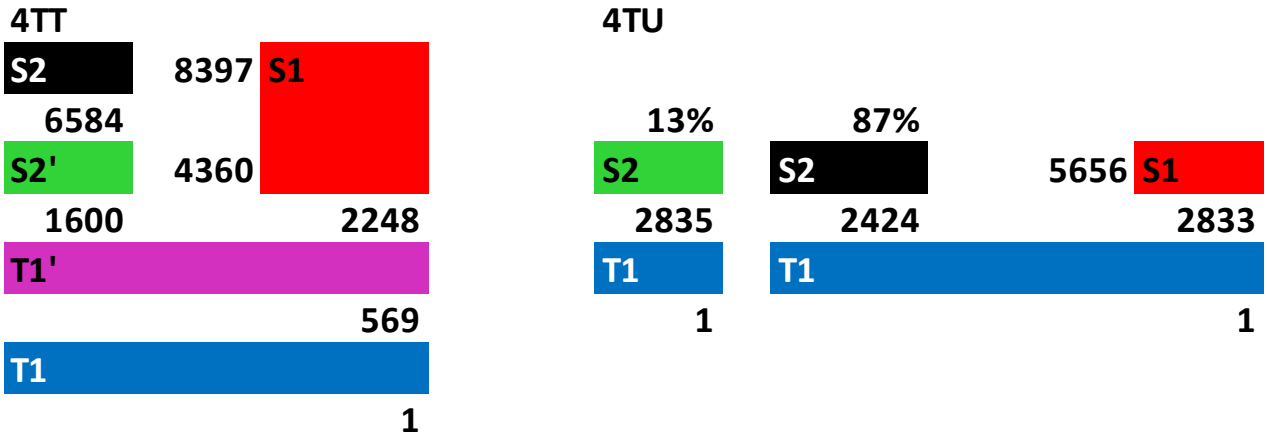

Figure S 2. Kinetic schemes used for the target analysis of 4TT (left) and 4TU (right) in PBS. All rate constants in ns^{-1}. Key 4TT: lifetimes: 67 fs (S2($1\pi\pi^*$), black), 168 fs (S'_2($^1\pi\pi^*$), green), 445 fs (S_1($^1n\pi^*$), red), 1.76 ps (T_1'($^3\pi\pi^*$), magenta) and long lived (T_1($^3\pi\pi^*$), blue). Key 4TU: lifetimes: major fraction (87%) 124 fs (S_2($^1\pi\pi^*$), black), 353 fs (S_1($^1n\pi^*$), red), and long lived (T_1($^3\pi\pi^*$, blue). Minor fraction (13%) 353 fs (S_2($^1\pi\pi^*$), green), and long lived (T_1($^3\pi\pi^*$, blue). Note that with the major fraction of 4TU a branching from S_2 has been assumed, with 30% of S_2 directly converting to triplet.

The quality of the fits is demonstrated in the eight representative panels in Figure S 3F-I and Figure S 4F-I. With 4TT, the root mean square error of the fits was 0.123 mOD, which can be judged when comparing the red and black curves in Figure S 3F-I. With 4TU, the root mean square error of the fits was 0.157 mOD, which can be judged when comparing the red and black curves in Figure S 4F-I.

In both 4TT and 4TU the Decay Associated Difference Spectra (DADS) depicted in Figure S 3C and Figure S 4C are complex, indicating that a complex kinetic scheme is necessary. The initial SADS is interpreted as S2 (black in Figure S 3B and Figure S 4B). The final SADS is equal to the final, long-lived DADS that is interpreted as T1 (blue in Figure S 3B,C and Figure S 4B,C). Several kinetic schemes have been tested, until we arrived at the schemes of Figure S 2 with well interpretable SADS that are in accordance with the theory.

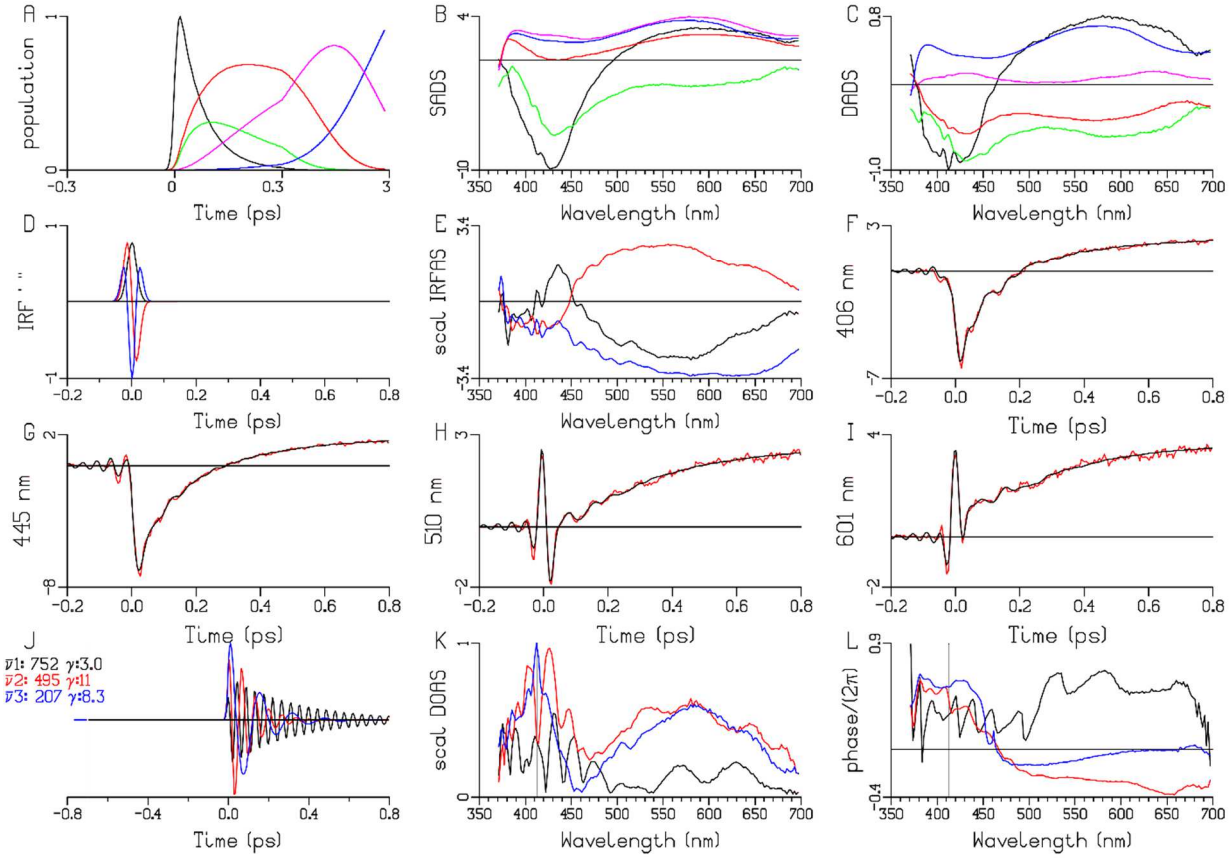

Figure S 3. DOAS analysis of 4TT in PBS solution excited with a 20 fs pulse centered at 330 nm. (A) Populations of the kinetic scheme used (*Figure S 2*A). Estimated SADS (B, in mOD) and DADS (C, normalized). Key A-C, lifetimes: 67 fs ($S_2(^1\pi\pi^*)$, black), 168 fs ($S'_2(^1\pi\pi^*)$, green), 445 fs ($S_1(^1n\pi^*)$, red), 1.76 ps ($T'_1(^3\pi\pi^*)$, magenta) and long lived ($T_1(^3\pi\pi^*)$, blue). (D) CA IRF 0th, 1st and 2nd derivative (black, red and blue) (E) IRFAS. Scaling of the IRFAS is such that the product of the IRFAS and the IRF derivative is the contribution to the fit. (F-I) Zoom from -0.2 ps to 0.8 ps (after the maximum of the IRF) of the 406, 445, 510, 601 nm data (in mOD, red) and the fit (black). (J-L) Overview of the estimated DOAS and phases. (J) Cosine oscillations with frequencies $\bar{\nu}n$ (in /cm) (where n is the DOAS number) and damping rates γ (in 1/ps) written in the legend at the left, using the appropriate color. Scaling of the DOAS is such that the product of the DOAS and the damped oscillation is the contribution to the fit. (K) Estimated DOAS (with number indicated in the legend at the far left). (L) Estimated phase profiles of the DOAS. The grey vertical lines at 413 nm in panels K and L are discussed in the main text.

In 4TT, the SE emission from S_2 (large negative amplitudes near 420 nm) disappears in two phases of 67 and 168 fs (black and green DADS in Figure S 3C). This is modelled by the $S_2 \rightarrow S'_2 \rightarrow T'_1 \rightarrow T_1$ pathway, where the final step $T'_1 \rightarrow T_1$ represents vibrational relaxation of the triplet state. During this vibrational relaxation ESA disappears around 440 and 640 nm, cf. the magenta DADS in Figure S 3C. This vibrational relaxation is also visible in the 4TT transient absorption data of Fig.1b in [4]. Additionally, 56% of S_2, and even 73% of S2', decays via the S_1 state. The thus estimated red SADS (Figure S 3B) shows positive ESA around 600 nm and 380 nm that support the interpretation of the red SADS as belonging to the S_1 state.

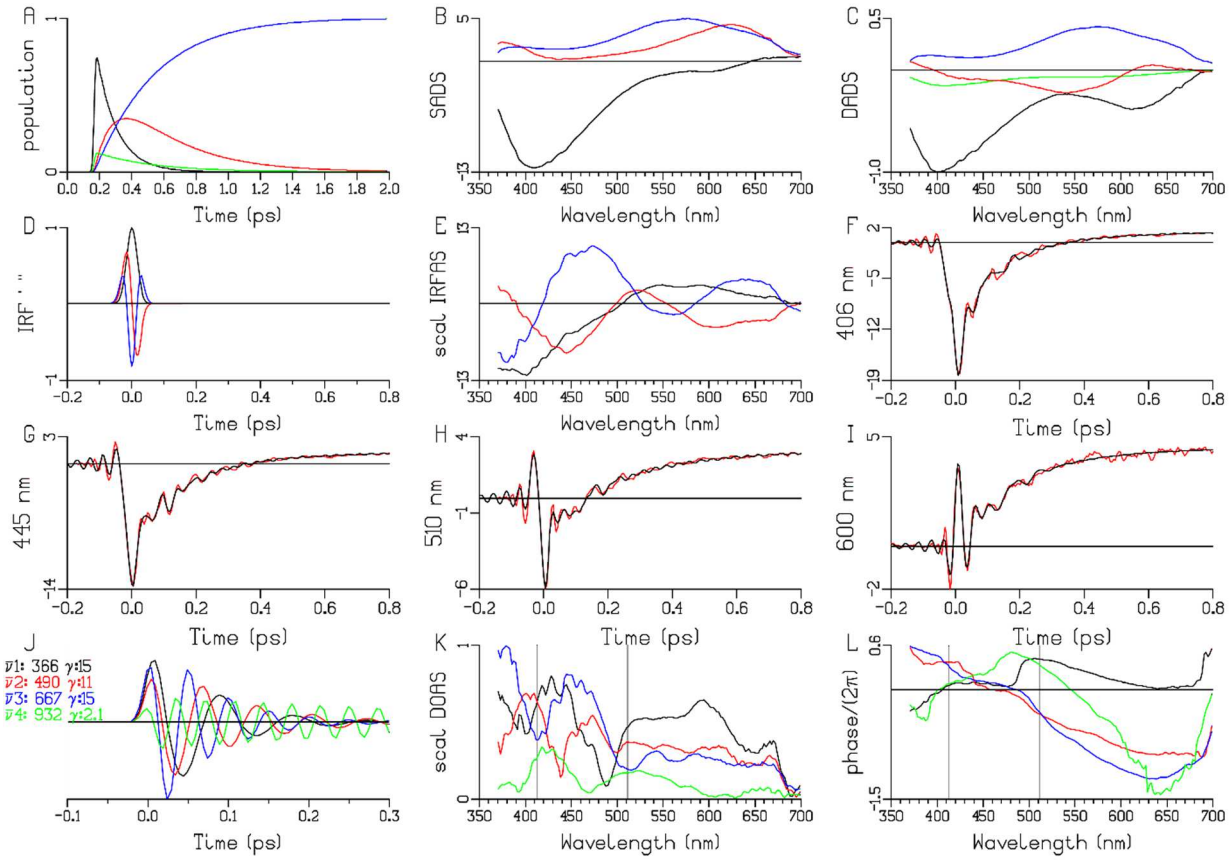

Figure S 4. DOAS analysis of 4TU in PBS solution excited with a 20 fs pulse centered at 330 nm. (A) Populations of the kinetic scheme used (*Figure S 2*B). Estimated SADS (B) and DADS (C). Key A-C, lifetimes: major fraction (87%) 124 fs (S2($1\pi\pi^*$), black), 353 fs ($S_1(^1n\pi^*)$, red), and long lived ($T_1(^3\pi\pi^*$, blue). Minor fraction (13%) 353 fs ($S_2(^1\pi\pi^*)$, green), and long lived ($T_1(^3\pi\pi^*$, blue). The SADS of black and green are equal. (D) CA IRF 0th, 1st and 2nd derivative (black, red and blue) (E) IRFAS. Scaling of the IRFAS is such that the product of the IRFAS and the IRF derivative is the contribution to the fit. (F-I) Zoom from -0.2 ps to 0.8 ps (after the maximum of the IRF) of the 406, 445, 510, 601 nm data (in mOD, red) and the fit (black). (J-L) Overview of the estimated DOAS and phases. (J) Cosine oscillations with frequencies $\bar{\nu}n$ (in /cm) (where n is the DOAS number) and damping rates γ (in 1/ps) written in the legend at the left, using the appropriate color. Scaling of the DOAS is such that the product of the DOAS and the damped oscillation is the contribution to the fit. (K) Estimated DOAS (with number indicated in the legend at the far left). (L) Estimated phase profiles of the DOAS. The grey vertical lines at 413 and 511 nm in panels K and L are discussed in the main text.

In 4TU the 353 fs decay process is decomposed in two components, green and red. The shape of the green DADS is identical to the shape of the black DADS (Figure S 4C), but the amplitude is much smaller. The green is assumed to represent a small fraction (13%) of more slowly decaying S_2, whereas the black DADS (124 fs) represents the major fraction (87%) of S2 that decays to S1. In turn S_1 decays to T_1 also in 353 fs. The red 353 fs SADS (Figure S 4B) shows positive ESA amplitude around 630 nm and 380 nm. These features evidence the interpretation of the red SADS as belonging to the S_1 state.

8. Target 4TU SADS analyses and assignments of the bands

The 4TU calculated decay path explanation is strongly supported by the good matching between the stimulated emission (SE) and photoinduced absorption (PA) estimations along the relaxation route and the experimental SADS signals. Figure S5 shows these correspondences, referring on the computational results depicted in Figure 2.

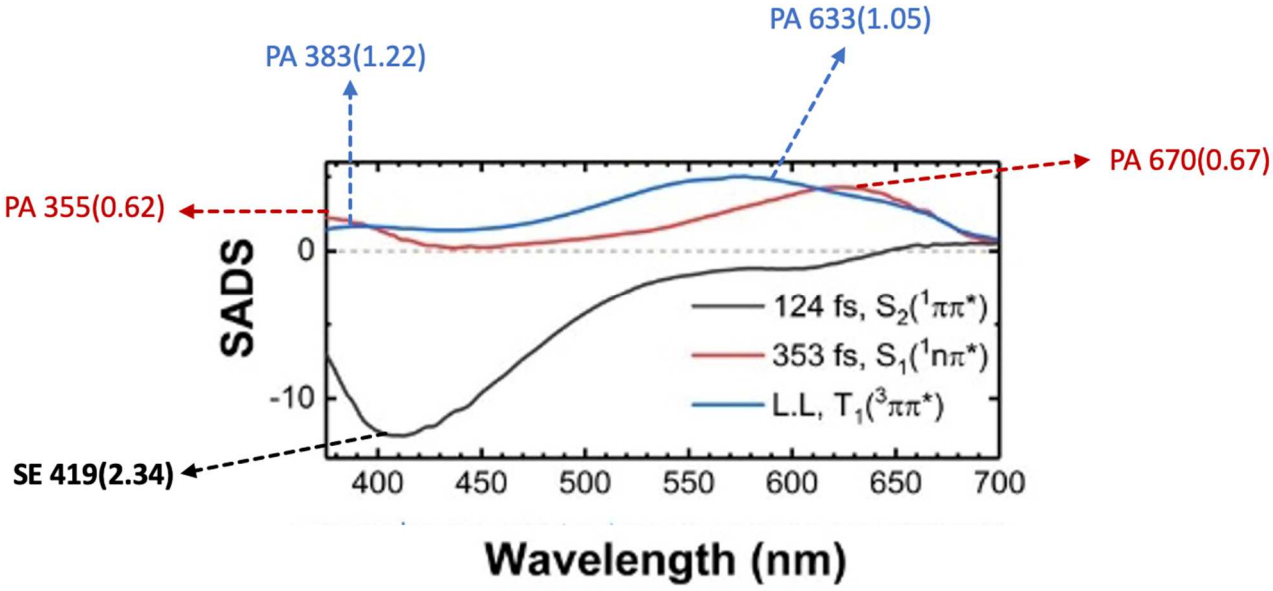

Figure S5. SADS black line, corresponding to the first time constant (124 fs), shows an intense negative band matching exactly with the reported SE value, calculated on top of the $Min_{TU}S_2(^1\pi\pi^*)$ and documented in Figure 2. The red line positive peaks lie in the same region of the PA calculated energy value, on top of the $Min_{TU}S_2(^1n\pi^*)$. The blue line should represent the final T_1 triplet population ($^3\pi\pi^*$): this is confirmed by the PA calculated signals, which are matching with the experimental bands.

References:

[1] R. Borrego-Varillas, D.C. Teles-Ferreira, A. Nenov, I. Conti, L. Ganzer, C. Manzoni, M. Garavelli, A. Maria de Paula, G. Cerullo, Observation of the Sub-100 Femtosecond Population of a Dark State in a Thiobase Mediating Intersystem Crossing, Journal of the American Chemical Society, 140 (2018) 16087-16093.
[2] I.H.M. van Stokkum, M. Kloz, D. Polli, D. Viola, J. Weißenborn, E. Peerbooms, G. Cerullo, J.T.M. Kennis, Vibronic dynamics resolved by global and target analysis of ultrafast transient absorption spectra, The Journal of Chemical Physics, 155 (2021) 114113.
[3] S.A. Kovalenko, A.L. Dobryakov, J. Ruthmann, N.P. Ernsting, Femtosecond spectroscopy of condensed phases with chirped supercontinuum probing, Physical Review A, 59 (1999) 2369-2384.
[4] C. Reichardt, C.E. Crespo-Hernández, Room-Temperature Phosphorescence of the DNA Monomer Analogue 4-Thiothymidine in Aqueous Solutions after UVA Excitation, The Journal of Physical Chemistry Letters, 1 (2010) 2239-2243.